Nanocrystalline pyrochlore bonded to proton exchange membrane electrolyte as electrode material for oxygen reduction

V. RAGHUVEER, B. VISWANATHAN*
*Department of Chemistry,Indian Institute of Technology, Madras, Chennai 600 036, India
E-mail: bvnathan@iitm.ac.in*

The nanocrystalline Pb-Ru pyrochlore prepared by reverse microemulsion method has been used as the cathode electro catalyst for oxygen reduction reaction in proton exchange membrane (Nafion 117) medium. The oxide particles prepared were found to have nanosized spherical as well as filament type particles. The nanocrystalline Pb-Ru pyrochlore was found to exhibit comparable electrocatalytic activity and stability with commercial platinum catalyst, for oxygen reduction reaction.
© *2005 Springer Science + Business Media, Inc.*

1. Introduction

Nanostructured materials are of great importance as they find applications in the field of optics, electronics, mechanics and catalysis [1]. In catalysis, they offer unique size-dependent property, a large surface to volume ratio and unusual chemical/electronic synergistic effect from ultra high component dispersion. There have been major studies on exploiting metal oxides as cathodes for the reduction of oxygen in fuel cells and batteries, since these materials can be expected to provide reversible pathway for oxygen reaction [2–5]. The development of less expensive oxide electro catalyst for the reduction of oxygen at lower potentials can have major economic consequences. Spinels such as Co_3O_4 and $NiCo_2O_4$ [2], large number of doped lanthanum cobaltites [5, 6] and lanthanum manganites [7] have been investigated for oxygen reduction. But these materials are restricted to alkaline medium as they undergo leaching in acid medium. Normally, the fuel cell operation prefers acid as electrolyte, since the formation of carbonates in the alkaline medium results in loss in fuel cell performance. The pyrochlore ($Pb_2Ru_2O_7$) was first identified by Horowitz [8, 9] as an active electro catalyst for oxygen reduction whose efficiency was considered to be comparable to that of the noble metals in alkaline medium. This pyrochlore material is also known to be stable in acids. These type of oxide electrodes are preferable as cathodes, especially in the Solid polymer electrolyte-Direct Methanol Fuel Cells (SPE-DMFC), because of being methanol tolerant. The most commonly employed acidic solid polymer electrolyte, Nafion 117, has the drawback of methanol permeation across the membrane [10–12], which poisons the platinum catalyst at the cathode. Hence, a methanol tolerant cathode is preferable.

The electrocatalytic activity of the pyrochlore for the oxygen reduction reaction depends on the Pb content on the B sub-lattice. The maximum activity was achieved for the composition $Pb_2Ru_{1.95}Pb_{0.05}O_{7-\delta}$ [13, 14]. Though enhancement in the activity for oxygen reduction was noticed when Pb-Ru pyrochlore was dispersed on the Vulcan XC 72 R carbon [15], even then the activity is significantly lower compared to that of the platinum catalyst. To improve further, we attempted to prepare the material in the nanocrystalline form. This is because; for the charge transfer reactions that involve majority carriers, the rate of charge transfer process across the interface depends on the surface concentration of the charge carriers (or density of states) of the electrodes [16–18], which can be altered suitably by transition metal ion substitution or by controlling the particle size. Recently, we have established a correlation between the methanol oxidation currents and the density of states of the electrode [19, 20], by suitable transition metal ion substitution and control of particle size. Since, the maximum activity for the oxygen reduction reaction was exhibited by the pyrochlore of composition $Pb_2Ru_{1.95}Pb_{0.05}O_7$, we believe that decreasing the particle size can enhance the rate of the oxygen reduction reaction further. This is because, the oxides when fabricated in nanocrystalline form, can be expected to exhibit altered electrochemical behaviors by virtue of an enhanced surface to volume factor as well as due to alterations in the density of states by introducing Shockley states in the diffuse space charge region inside the solid.

To the best of our knowledge, no prior work on nanocrystalline Pb-Ru pyrochlore for oxygen reduction reaction has been reported. Here we report the synthesis of nanocrystalline pyrochlore by reverse microemulsion method and its electrocatalytic activity for oxygen reduction reaction in proton exchange membrane medium.

2. Experimental procedure

2.1. Preparation of the nanocrystalline pyrochlore

The preparation of the nanocrystalline Pb-Ru pyrochlore material reported is based on the reverse micellar method. The stoichiometric amounts of lead nitrate (s.d. fine-chem Ltd.) and Ruthenium chloride trihydrate (Hindustan platinum Ltd.), required to prepare the pyrochlore of composition $Pb_2Ru_{1.95}Pb_{0.05}O_7$, were dissolved in 67 ml of water. This aqueous solution was added from the burette slowly into 0.1 M AOT/n-heptane mixture with vigorous stirring, to prepare water in oil microemulsion I. The surfactant Sodium dioctyl sulfosuccinate (AOT) and n-heptane were obtained from Loba Chemie and CDH respectively. To facilitate the mixing of the salt solution in the AOT/n-heptane mixture, ultrasonication was carried out for 10 min. The molar concentration of lead nitrate and ruthenium chloride in the microemulsion I, were 8×10^{-4} M and 7.9×10^{-4} M respectively. Microemulsion II was prepared by adding KOH in 0.1 M AOT/n-heptane mixture with vigorous stirring. The molar concentration of KOH in microemulsion II was 5.9×10^{-2} M. A Water/AOT ratio of 15 was maintained in both microemulsions. Microemulsions I and II were mixed together vigorously with a magnetic stirrer at room temperature. After few seconds, the mixed microemulsions become turbid because of the formation of particles. The microemulsion reaction proceeded for 2 h, (enough reaction time) under the vigorous agitation. The particles formed in the microemulsions were not sedimented because of the adsorption of the surfactant molecules on the surface of particles and the formation of the stable dispersion of particles. After the reaction, acetone was added to break the microemulsion structure and to cause sedimentation of the Pb-Ru hydroxide particles. The sedimented Pb-Ru hydroxide particles were washed with acetone and water successively to remove the surfactant molecules and sodium ions from particle surfaces. During the washing process, centrifugal force (4500 rpm for 10 min) was applied to the samples to shorten the sedimentation time. The washed Pb-Ru pyrochlore particles were dried in air oven maintained at 120°C for 2 h and crushed by mortar and pestle. Then, the Pb-Ru hydroxide particles were calcined at 500°C for 2 h in air. In the present work, the nanocrystalline Pb-Ru pyrochlore is coded as RMEpyro.

2.2. Characterization technique

The XRD measurements for the powdered samples of the nanocrystalline pyrochlores were obtained using a Philips PW 1130 at room temperature. The radiation used is Ni filtered Cu K_α ($\lambda = 1.5405$ Å). The C, H and N analysis were obtained using Heraeus CHN analyzer. The microscopic analysis of the nanocrystalline oxide was obtained using Philips CM12/STEM, Scientific and Analytical Equipment. The sample was dispersed in ethanol by sonification and dropped on to a carbon grid and imaged at 120 kV.

2.3. Gas diffusion electrodes

The gas diffusion electrodes were composed of a pair of carbon layers (a gas supply layer and an active layer) with a carbon cloth (current collector) sandwiched in between. The gas diffusion electrode was prepared by mixing the Pb-Ru pyrochlore oxide catalyst with carbon (Vulcan XC 72R) in 1:3 ratio and suspended in water with 5% Nafion. For, the commercial catalyst, the platinum supported carbon (20% Pt/C, Arora Mathey) was taken as such and suspended in water and 5% Nafion solution. The mixture was thoroughly homogenenized with a ultrasonicator before and a dilute PTFE dispersion was added, for 30 min. The active layer contains 20 wt% of PTFE. The presence of Nafion in the mixture will enhance the mixed electronic-ionic contact of the electrode, in order to provide necessary interface between catalyst, reactant, and electrolyte. The
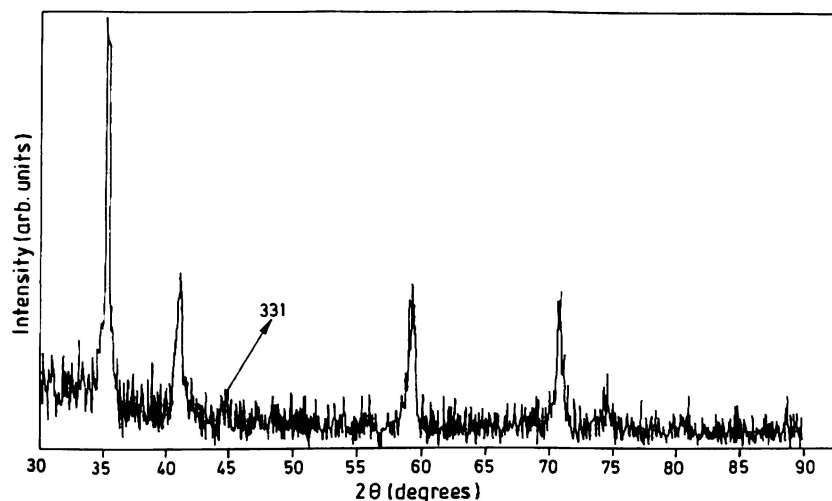

Figure 1 X-ray diffraction pattern obtained for $Pb_2Ru_{1.95}Pb_{0.05}O_{7-\delta}$ nano particles prepared by reverse micellar method.

6250

resulting semi-solid paste was then spread onto the previously treated Teflon containing uncatalysed carbon coated carbon cloth and leveled by roller.

2.4. Membrane electrode assembly

The half-cell assembly and the preparation of MEA were made based on the literature reported elseshere [15]. The carbon cloth containing the catalyst layer side was bonded to a previously treated Nafion 117 membrane by placing the Nafion membrane on top of the coated surface, the assembly was then hot pressed for 3 min. The other side of the carbon cloth that contains Teflon containing uncatalysed carbon was used as gas diffusion layer, through which gas diffuses to the catalytic active sites. The geometric area of the carbon cloth with the catalyst layer used in the present study is 2.5 cm^2. The membrane and electrode were placed between two graphite plates, which were then clamped together with stainless steel bolts. One of the graphite plates with grooves, having gas diffusion layer has a hollow cavity with gas inlet and outlet used to feed the reactant gas, oxygen or nitrogen in this study, to the porous electrode. The other graphite plate has holes, which was attached with acid resistant rubber washer, is in contact with 2.5 M sulphuric acid reservoir to provide a source of protons to be transported through the membrane and consumed in the porous electrode. The pretreated Nafion 117 membrane was used as the solid polymer electrolyte in the membrane electrode assembly. The temperature of the electrochemical cell was suitably monitored by applying power from the dimmerstat to the heating coil present in the cell. The whole electrochemical half cell was covered with the asbestos tape to prevent heat dissipation and to maintain the temperature of the electrochemical cell. The flow rates of the gases (oxygen and nitrogen) were controlled using mass flow controller.

2.5. Electrochemical measurements

The electrochemical oxygen reduction was carried out using cyclic voltammetry (Potentioscan Wenking POS 73). The reference and counter electrodes used are Ag/AgCl and Pt foil (1.5 cm^2), respectively. The concentration of the sulphuric acid in the reservoir used is 2.5 M. The scan rate of 25 mV/s was chosen for recording the cyclic voltammogram. The electrolyte reservoir was deaerated with bubbling nitrogen gas before use. The nitrogen gas was fed to the gas diffusion layer from the rear side for 1 h at the flow rate of 12 ml/min to flush any adsorbed oxygen present on the oxide surface, before recording the voltammogram. For the electrochemical studies, the flow rate of nitrogen and oxygen gas was fixed to 12 ml/min.

3. Results and discussion

3.1. X-ray diffraction characterization

Fig. 1 shows the X-ray diffraction (XRD) pattern of the nanocrystalline Pb-Ru pyrochlore. The pattern obtained agreed with the one reported in the JCPDS standard (File no. 34-472). The pattern indicates single-phase pyrochlore with well-defined superstructure reflections corresponding to (331) plane at 2θ (44.778 Å). The XRD peaks in Fig. 1 are characteristically broader than normally obtained for large crystallites, which is expected for nanosized cyrstallites.

3.2. CHN analyses

Since, the oxide nanoparticles were prepared by the chemical method using an organic surfactant (Sodium dioctylsulfosuccinate); there is a possibility of the organic impurities (C, H and N) present on the oxide particle surface, which may have negative effect on the
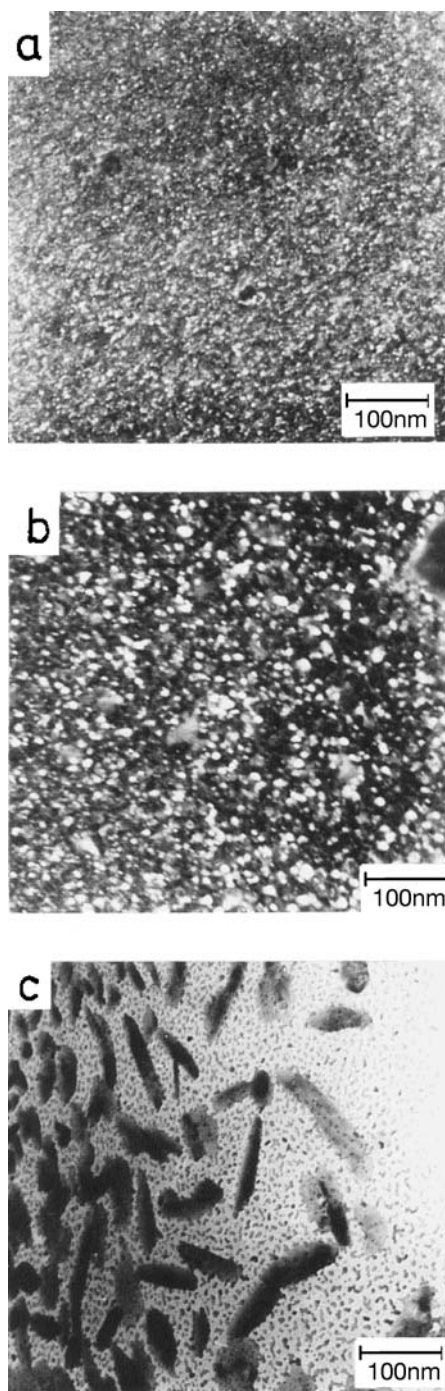

Figure 2 Transmission electron micrographs of $Pb_2Ru_{1.95}Pb_{0.05}O_{7-\delta}$ oxide nano particles prepared by reverse micellar method showing (a and b) ultra fine spherical particles (c) elongated filament type particles.

catalytic performance. In order to ensure the absence of organic surface impurities and complete removal of surfactant from the nanocrystalline Pb-Ru pyrochlore oxide sample, the CHN analysis was carried out for the pyrochlore sample after the calcination. The percentages of C (<0.5%), H (<0.4%) and N (Nil) are considerably low, thus, confirming the complete removal of the surfactant species and almost absence of organic impurities.

3.3. Transmission electron microscopic characterization

Fig. 2 shows the TEM image of Pb-Ru pyrochlore oxide particles, recovered from reverse micelles, taken in different regions, in which the ultra fine dispersion of oxide particles can be seen. The overall particle size ranges from 1–20 nm. In Fig. 2a, the particle sizes were in the range 2–5 nm, which implies that the size of the oxide particles formed in the microemulsion is of the same order of the water droplet size. Fig. 2b shows particle agglomerates about sizes >15 nm, which is greater than the size of the water droplets. This means that the Pb-Ru hydroxide particle size of 2–5 nm grow to oxide particles of >15 nm during the calcination process at 500°C for 2 h or during the intermicellar exchange, the particle grows to a size which may be greater than that of size of the water droplet. Elongated filament type particles were also observed, which is
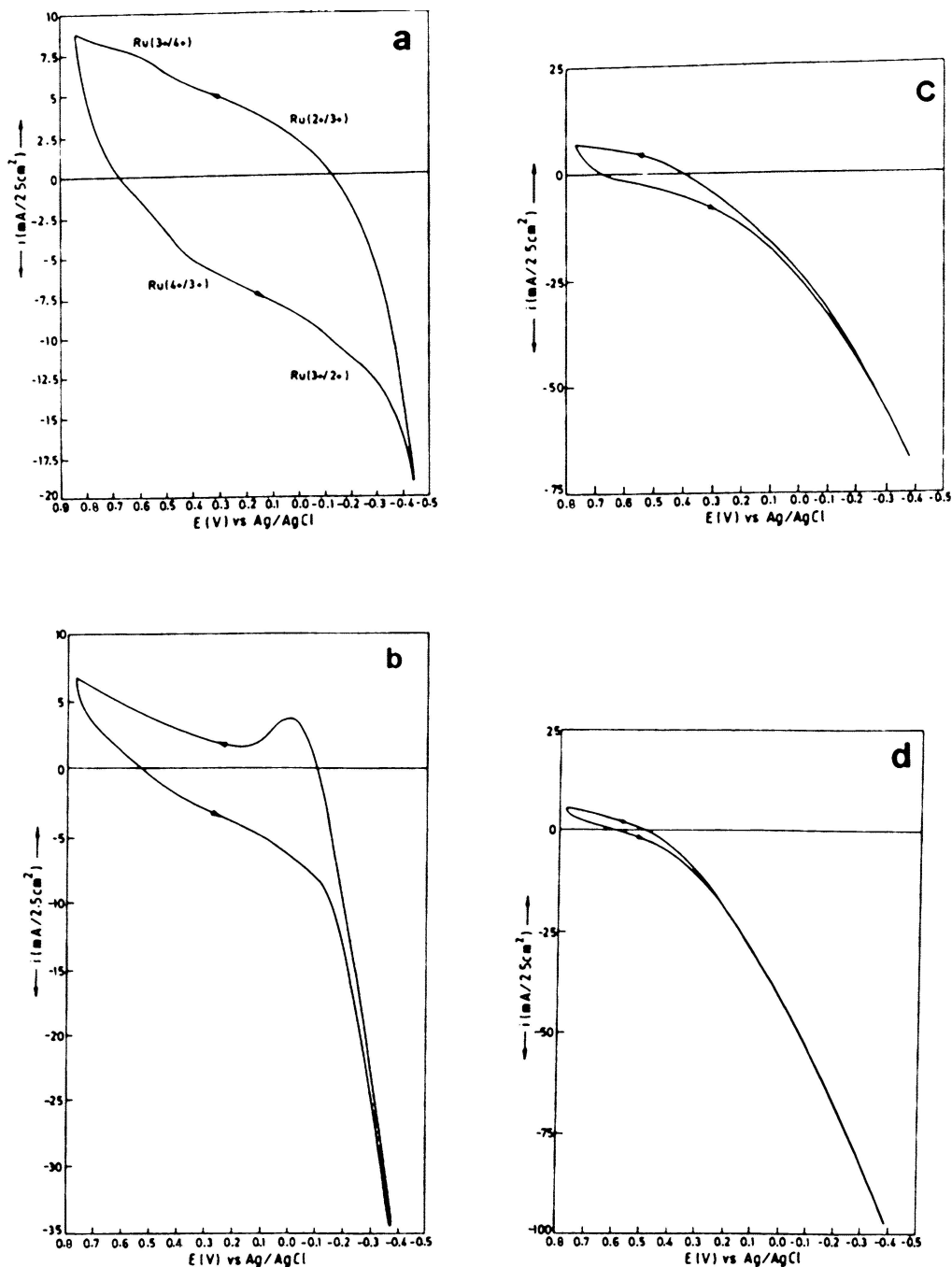

Figure 3 Cyclic voltammogram obtained for (a) nanocrystalline Pb-Ru pyrochlore oxide (RMEpyro) sample and (b) commercial platinum (20%Pt/C) bonded to Nafion 117 membrane in the presence of nitrogen gas, (c) nanocrystalline Pb-Ru pyrochlore oxide sample (RMEpyro) and (d) commercial platinum (20%Pt/C) bonded to Nafion 117 membrane in the presence of oxygen gas on the back side of the electrode at a scan rate of 25 mVs^{-1} at RT.

evident from Fig. 2c. The size of the elongated filament type particles is of 100 nm. The formation of this type of elongated filament particles may be due to the high water content (>20–30%). At higher water contents, significant percolation of the micellar domains might occur, leading to a mixture of liquid crystalline phases [21, 22]. The nanocrystalline Pb-Ru oxide sample recovered from these systems showed spherical as well as elongated particle morphologies as seen from Fig. 2c.

3.4. Electrochemical oxygen reduction reaction

The nanocrystalline oxide sample is found to be stable in the test cell where the catalyst was bonded to one side of the Nafion 117 membrane and 2.5 M sulfuric acid solution contacted to the other side of the membrane. The loading of the Pb-Ru pyrochlore and platinum on the gas diffusion electrode was obtained by UV-Vis spectrophotmetry. The loading of pyrochlore and Pt in the GDE was found to have 1.8 mg/2.5 cm^2 and 0.6 mg/cm^2 respectively. Care was taken to remove the adsorbed oxygen on the electrocatalyst surface by passing the nitrogen gas to the gas diffusion layer from the rear side for 1 h, before recording the voltammograms. The cyclic voltammograms taken in the presence of nitrogen on the backside of the electrocatalyst in the potential range of +0.8 to −0.5 V *vs* Ag/AgCl, at room temperature, is shown in Fig. 3a (RMEpyro) and Fig. 3b (commercial 20%Pt/C). The redox peak potentials obtained for the nanocrystalline Pb-Ru pyrochlore (RMEpyro) (Fig. 3a) are in good agreement with peak potentials reported in the literature [10, 11]. The observed peaks are characteristically broader, which is normally expected for the nanocrystallites. For the commercial platinum catalyst (20% Pt/C), the presence of Pt (Fig. 3b) in the gas diffusion electrode is evident from the broad peak at –0.2 V vs Ag/AgCl, which is due to the hydrogen desorption from Pt surface. On introduction of the oxygen gas from the rear side of both the electrode materials (RMEpyro and commercial platinum catalyst), the open circuit voltages shifted to a more positive equilibrium potential, indicating the establishment of the oxygen reduction reaction at the protonated oxide surface. The cyclic voltammogram obtained for Pb-Ru pyrochlore and commercial 20% Pt/C (Arora Mathey), in the presence of oxygen, is shown in Fig. 3c and d respectively. The higher current response in the presence of oxygen compared to that of the nitrogen, suggests that the oxygen reduction reaction is taking place. The current increases with the increase in the cathodic potential. The magnitude of the current during the forward and reverse scan is almost equal, indicating the absence of poisoning by the peroxo intermediate formed during the electroreduction of oxygen. The current density at +0.2 V vs Ag/AgCl, during the forward cathodic scan provides a measure of electrocatalytic activity; it decreases with decrease in the oxygen pressure to the value shown for the nitrogen curve. The electrocatalytic activity exhibited by the nanocrystalline Pb-

Ru pyrochlore (14 mA) was found to be comparable with that of the commercial platinum catalyst (14 mA). The oxygen reduction onset potential observed for the nanocrystalline pyrochlore, RMEpyro (Fig. 3c) when used as cathode was found to be comparable with that of the commercial platinum (Fig. 3d). Upon increasing the operating temperature to 70°C, the enhancement in the oxygen reduction was observed, which could be due to the decrease in the charge transfer resistance.

The Pb-Ru pyrochlore sample of same composition prepared by the conventional ceramic method (Fig. 4) exhibited lower activity (1.6 mA) for the same loading of oxide (1.8 mg/2.5cm^2) in the gas diffusion mode. By conventional ceramic method, the oxide particles will have higher particle size that is because of the high temperature being adopted for the calcination, during which the particles will undergo sintering. The higher particle size oxide particle will have low surface to volume ratio and low density of surface states at the space charge region and hence leads to exhibit lower activity [13]. In the case of nanocrystalline oxide sample (RMEpyro), the higher activity exhibited by the oxide sample could be due to the increase in the surface to volume ratio and higher density of surface states in the space charge region. This is because, as valence and conduction bands evolve from the initial diatomic states, upon the extension of the bonding in the lattice, unbound and partially bound surface (dangling or broken bonds) atoms or surface atoms with strained bonds introduce states within the band gap [23]. Since the number of broken bonds or dangling bonds is higher for the oxide with smaller crystallite size, therefore the
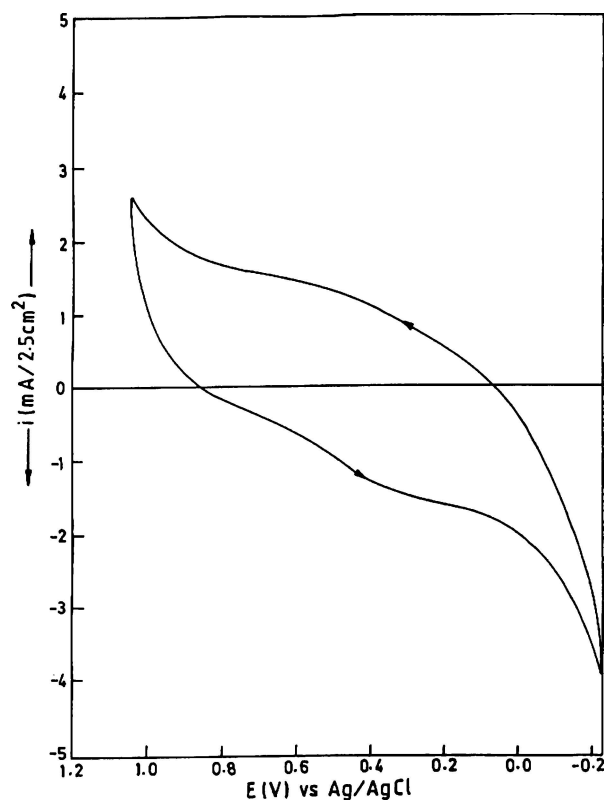

Figure 4 Cyclic voltammogram obtained for Pb-Ru pyrochlore oxide sample prepared by conventional ceramic method bonded to Nafion 117 membrane in the presence of oxygen gas on the back side of the electrode at a scan rate of 25 mVs^{-1} at RT.

density of surface states is increased in the band gap thus leading to enhanced activity.

3.5. Chronoamperometry

Fig. 5 shows the chronoamperometric responses of the nanocrystalline Pb-Ru pyrochlore sample and that of commercial platinum electrodes for the oxygen reduction at +0.2 V vs Ag/AgCl for 1.5 h, at room temperature and 70°C. These studies are used to evaluate the stability of the electrode toward poisoning intermediate, such as peroxo species, during the oxygen reduction reaction. The decrease in the activity, after polarizing the electrode at +0.2 V vs Ag/AgCl, is more pronounced in the case of commercial platinum catalyst compared to that of the nanocrystalline Pb-Ru pyrochlore (RMEpyro) oxide sample. The higher rate of deactivation of the platinum catalyst is because of the formation of oxygen reduction intermediate (peroxo species), which poisons the catalyst [24]. Whereas, the lower rate of deactivation exhibited by the nanocrystalline pyrochlore sample (RMEpyro), at 25 and 70°C, indicates the tolerance of pyrochlore toward poisoning intermediates. At 25°C, though the activity exhibited by the nanocrystalline pyrochlore is slightly lower than platinum, but, the stability seems to be better than the platinum catalyst. Whereas, at 70°C, the nanocrystalline pyrochlore (RMEpyro) seems to exhibit better activity and stability compare to that of the commercial platinum cathode electrocatalyst. This activity enhancement is due to the decrease in the charge transfer resistance upon increasing the operating temperature. These results reveal that the nanocrystalline Pb-Ru pyrochlore exhibits better electrode stability toward poisoning intermediates formed during the oxygen reduction reaction compared to that of the commercial platinum catalyst.

4. Conclusions

In conclusion, we report the synthesis of nanocrystalline Pb-Ru pyrochlore by reverse microemulsion method (RMEpyro). The XRD and TEM studies show the nanocrystalline nature of the Pb-Ru pyrochlore with spherical nanoparticles and elongated type particle morphology. The nanocrystalline Pb-Ru pyrochlore (14 mA, 1.8 mg/2.5 cm^2) exhibits comparable activity with that of the commercial platinum catalyst (14 mA, 0.6 mg/2.5 cm^2), for oxygen reduction reaction in the proton exchange membrane medium at 25°C. The enhancement in oxygen reduction reaction current for the RMEpyro and platinum electrocatalyst upon increasing the operating temperature is due to the decrease in the charge transfer resistance. The chronoamperometric measurements reveal that the nanocrystalline pyrochlore exhibits better electrode stability toward poisoning intermediates at 25 and 70°C, compared to that of commercial platinum electro catalyst for oxygen reduction reaction.

Figure 5 Chronoamperometric responses of nanocrystalline Pb$_2$Ru$_{1.95}$Pb$_{0.05}$O$_{7-\delta}$ oxide sample (RMEpyro) and commercial platinum catalyst (20% Pt/C) for the oxygen reduction polarizing potential at +0.2 V vs Ag/AgCl in the 12 ml/min flow rate of oxygen gas from the back side of the electrode at different operating temperatures.

References

1. J. A. COWEN, B. STOLZMAN, R. S. AVERBACK and J. HANH, *J. Appl. Phys.* **61** (1987) 3317.
2. D. B. HIBBERT and A. C. C. TSEUNG, *J. Electrochem. Soc.* **125** (1978) 75.
3. A. C. C. TSEUNG and K. L. K. YEUNG, *J. Electrochem. Soc.* **125** (1978) 1003.
4. R. MANOHARAN and A. K. SHUKLA, *Electrochim. Acta.* **30** (1985) 205.
5. Y. SHIMIZU, K. UEMURA, H. MATSUDA, N. MIURA and N. YAMAZOE, *J. Electrochem. Soc.* **137** (1990) 3430.
6. S. MULLER, F. HOLZER, O. HAAS, C. SCHLATTER and C. COMNINELLIS, *Chimia.* **49** (1995) 27.
7. M. HAYASHI, T. HYODO, N. MIURA and N. YAMAZOE, *Electrochemistry*, **68** (2000) 112.
8. H. S. HOROWITZ, J. M. LONGO and J. L. HABERMANN, US Patent **4**(146) (1977) 458.
9. H. S. HOROWITZ, J. M. LONGO and J. T. LEWANDOWSKI, US Patent, **4**(163) (1997) 707.
10. P. S. KAURANEN and D. SKOU, *J. Electroanal. Chem.* **408** (1996) 189.
11. K. SCOTT, W. M. TAAMA, P. ARGYROPOLOUS and K. SUNDMACHER, *J. Power Sources.* **83** (1999) 204.
12. J. W. LONGO, R. M. STROUND, K. E. SWIKURLYONS and D. R. ROLISON, *J. Phys. Chem. B.* **104** (2000) 9772.
13. H. S. HOROWITZ, J. M. LONGO and H. H. HOROWITZ, *J. Electrochem. Soc.*, **130** (1983) 1851.
14. J. B. GOODENOUGH, R. MANOHARAN and M. PARANTHAMAN, *J. Am. Chem. Soc.* **112** (1990) 2076.
15. J.-M. ZEN, R. MANOHARAN and J. B. GOODENOUGH, *J. Appl. Electrochem.* **22** (1992) 140.
16. H. GERISCHER, *Electrochim. Acta*, **35** (1990) 1677.
17. R. MEMMING, *Solid State Ionics*, **94** (1997) 131.
18. A. M. KUZNETSOV and J. ULSTRUP, *Electrochim. Acta.* **45** (2000) 2339.
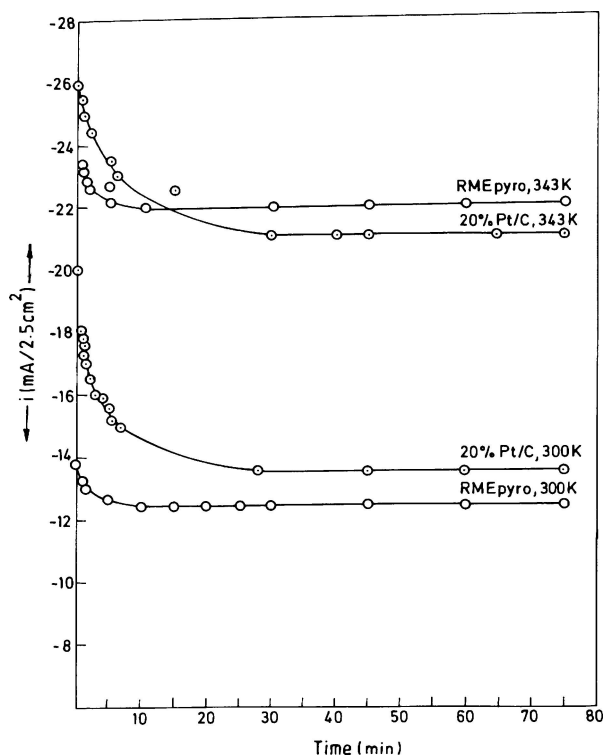19. V. RAGHUVEER and B. VISWANATHAN, *Fuel Chemistry Division Preprint*, **46** (2001) 461.

20. V. RAGHUVEER and B. VISWANATHAN, *Fuel* **81** (2002) 2191.
21. A. J. ZARUR and J. Y. YING, *Nature* **403** (2000) 65.
22. A. J. ZARUR, H. H. HWU and J. Y. YING, *Langmuir* **16** (2000) 3042.
23. A. J. NOZIK, in "Photoeffects at semiconductor-electrolyte interfaces" (ACS Symposium Series, Washington, DC, 1981).
24. L. D. BURKE, J. J. CASEY, J. A. MORRISSEY and J. F. O'SULLIVAN, *J. Appl. Electrochem.* **24** (1994) 30.